Lawrence Berkeley National Laboratory
LBL Publications

Title

3ω techniques for measurement of volumetric heat capacity and anisotropic thermal conductivity of a solution processable, hybrid organic/inorganic film, Te-PEDOT:PSS

Permalink

https://escholarship.org/uc/item/6xs1b47w

Journal

Journal of Applied Physics, 131(10)

ISSN

0021-8979

Authors

Forsythe, Carlos
Gordon, Madeleine P
Urban, Jeffrey J

Publication Date

2022-03-14

DOI

10.1063/5.0079328

Peer reviewed

eScholarship.org Powered by the California Digital Library
University of California

3ω Techniques for Measurement of Volumetric Heat Capacity and Anisotropic Thermal Conductivity of a Solution Processable, Hybrid Organic/Inorganic Film, Te-PEDOT:PSS

Carlos Forsythe, Madeleine P. Gordon, Jeffrey J. Urban

The Molecular Foundry, Lawrence Berkeley National Laboratory, Berkeley, CA 94720, USA.

Abstract

Measuring the thermal properties of anisotropic films of hybrid materials poses a challenge to existing metrology techniques. We have developed a new approach for measuring the volumetric heat capacity and anisotropic thermal conductivity of these systems using the 3ω method. While there exist many avenues for measuring the thermal properties of thin films, most carry with them difficult requirements such as smooth surfaces or advanced lithography. Here we present measurements of a film's in-plane and cross-plane conductance and its volumetric heat capacity using relatively simple sample configurations, each requiring a single heater. For the measurement of volumetric heat capacity, we present a new model fitting method, relying on a standard film-on-substrate configuration. For the measurement of in-plane thermal conductance by 3ω, we have developed the use of an embedded micro-wire heater in suspended drop cast films, allowing for a 12 μm wide heater without the need for advanced lithography. We also expose the surprisingly significant effect of thermal radiation in the suspended film measurement and its associated error. Our measurements reveal a large anisotropy in the thermal conductivity of our test material, Te-PEDOT:PSS, of $k_{in\text{-}plane}/k_{cross\text{-}plane}=19$, consistent with the nanoscale morphology of the material.

Introduction

Thermal characterization of films of many new materials remains difficult, generally due to their surface characteristics, morphology, or specific chemistry. Often, the thermal properties of these materials represent a key metric of their viability, especially in the field of energy generation and storage. Nanostructured materials commonly exhibit anisotropic thermal conductance, creating a need for both in-plane and cross-plane measurement of films. The 3ω method is especially attractive for this purpose, due to its use of a single metallic sensor, making sample preparation and measurement relatively easy. Here, we present a novel 3ω method of measuring the volumetric heat capacity of a film which relies on a standard film-on-substrate geometry. We further present a method for embedding a micro-wire heater onto a suspended film for the purpose of measuring in-plane thermal conductance by 3ω, where a commonly used evaporated heater is not viable due to the films rough surface and water-solubility.

There are 2 primary categories of thermal measurement for thin films: 3ω electrical measurements and laser-based thermoreflectance measurements[1]. While laser based techniques such as time-domain thermoreflectance and frequency-domain thermoreflectance require relatively simple sample preparations, they have strict requirements that make their use impossible from many solution processable materials. A primary limiter is the need for smooth material surfaces, with roughness ideally under 15 nm[2], which excludes many materials. There are thermoreflectance techniques which allow for the measurement of in-plane thermal conductivities of films, but they carry the requirement $k_{in\text{-}plane} > 5$ W/mK[3]. This especially limits application to polymers and their nanocomposites, which can struggle to reach a thermal conductance of this order[4]. On top of these sample restrictions, the required laser systems

for thermoreflectance measurements are expensive and require considerable maintenance. For these reasons, the 3ω method, though it often requires more difficult sample preparation, can generally be implemented easier and more cheaply.

The 3ω measurement is a relatively simple electronic measurement, but must be paired with a carefully designed sample and appropriate model in order to obtain accurate results[5–8]. The 3ω measurement relies on a thin metallic heater, which is affixed to the material of interest, and acts as both a heater and thermometer. An AC current with frequency ω, is passed through the heater, inciting a temperature oscillation, ΔT, at frequency 2ω. This temperature oscillation causes the heater resistance to oscillate in kind, which itself interacts with the oscillating current to create a voltage signal at frequency 3ω, which can be measured to calculate ΔT. Both the amplitude and phase of ΔT, and its relationship to ω, are indicative of the thermal properties of the medium surrounding the heater, however, the exact relationship is dependent on the sample configuration. Moreover, different sample configurations are inherently sensitive to different material properties.

Suspended film measurements are especially sensitive to $k_{in\text{-}plane}$, as transient heat waves induced by the heater are forced along the film plane in order to dissipate. However, a downside of using the 3ω method to measure $k_{in\text{-}plane}$ on a suspended film, is that the measurement requires a separate determination of the material's volumetric heat capacity, C_v. To meet that need, we pair the suspended 3ω measurement with a separate measurement, which allows for the determination of both C_v and $k_{cross\text{-}plane}$ through a novel model fitting analysis. In contrast to previously reported methods of determining C_v by 3ω[9,10], this technique relies on a very simple and standard device configuration, a film supported by a substrate, with a single wide heater atop the stack.

The suspended film measurement used here, for determining $k_{in\text{-}plane}$, is similarly straightforward[11]. Though the film is suspended, we use only a single heater, and there are no specific requirements on the thermal dissipation at film's supported edge. This differs from other methods which require axillary heaters or careful thermal grounding at the film boundaries in order to measure $k_{in\text{-}plane}$[8,9,12,13]. One hurdle that remains however, is the need for thin heaters, potentially thinner than achievable with metallic deposition by shadow mask. We have developed the use of a Pt micro-wire heater embedded into our material which sidesteps the burden of more advanced lithography. Pt is ideal for this use due to its high temperature coefficient of resistance, which increases its sensitivity as a temperature sensor in the 3ω measurement.

Discussion of model material, Te-PEDOT:PSS

To demonstrate these techniques, we measure Te-PEDOT:PSS, a bulk mesh of tellurium nanowires coated with poly(3,4- ethylenedioxythiophene) polystyrene sulfonate. Te-PEDOT:PSS functions as a thermoelectric material, owing to its high Seebeck coefficient and high electrical conductivity. However, the in-plane thermal conductivity of a drop cast film of Te-PEDOT:PSS, also relevant to its function as a thermoelectric material, remains absent from literature. The surface is too rough and its in-plane thermal conductivity is too low for thermoreflectance techniques. Measuring in-plane thermal conductance by 3ω requires a thin heater. However, given the film roughness and the material's water-solubility, applying advanced lithography and metallic deposition to fabricate such a heater is overly burdensome. By using a Pt micro-wire heater, we can measure the in-plane thermal conductivity of this material.

Our films are formed by drop casting an aqueous solution of Te-PEDOT:PSS in water. In order to boost anisotropic effects resulting from the Te nanowire structure, we have minimized the amount of unbound PEDOT:PSS in these materials through centrifugation. This minimization results in a low electrical conductivity of the dried Te-PEDOT:PSS film of 10 S/m. By modulated differential scanning calorimetry (MDSC)[14], we measure the heat capacity of our films to be 0.21 J/gK, which matches that of bulk Te (0.20-0.22 J/gK)[15] and is much lower than the organic component (~2 J/gK)[16,17], indicating that by mass, Te is the dominant component. We measure their density as 3.1 g/cm^3, half that of bulk Te (6.2 g/cm^3)[15] indicating that the Te nanowires form a mesh with considerable gaps, filled either by vacuum or unbound organic material.

We image our films by scanning electron microscope to reveal any ordering of the nanowires (Fig 1a). In a previous study, we have measured the wires to have an average length of 4.2 um and diameter of 57 nm[18]. Here, we observe some short range ordering on the sub-100 μm scale, with adjacent wires having the same rotational orientation within the film, forming grains. However, these grains of closely packed, rotationally aligned nanowires are relatively small, and as we can see at the broken edge of the film, they do not even persist through its thickness. At scales larger than 100 μm, the only apparent long range ordering within the film is a tendency for nanowires to orient in-plane, i.e. they lie flat. Therefore, at the macroscopic level, we expect the film to have equivalent thermal conductivity in every in-plane direction, as there is no specific preferred in-plane orientation to the nanowires. Along the cross-plane direction (perpendicular to the film), the thermal conductivity should differ, as the Te nanorods are generally oriented perpendicular to this direction.

Due to the underlying morphology of these films, we expect that the thermal conductivity is higher in the in-plane direction than cross-plane. Single wire measurements of the Te-PEDOT:PSS hybrid have shown that the Te core rather than organic shell is the primary conduit of thermal transport along the wire[19]. In a film of composite material, we expect that interfacial resistances between phases (i.e. between individual nanowires and surrounding polymer) will strongly affect overall thermal conductivity[20,21]. Heat flow traveling in-plane will generally be able to travel farther without scattering at these interfaces, aided by thermally conductive Te nanorods which have some degree of alignment with the direction of transport. In the cross-plane direction, the thin Te nanorods are uniformly oriented perpendicular to heat flow, resulting in much more densely packed scattering interfaces along this direction.

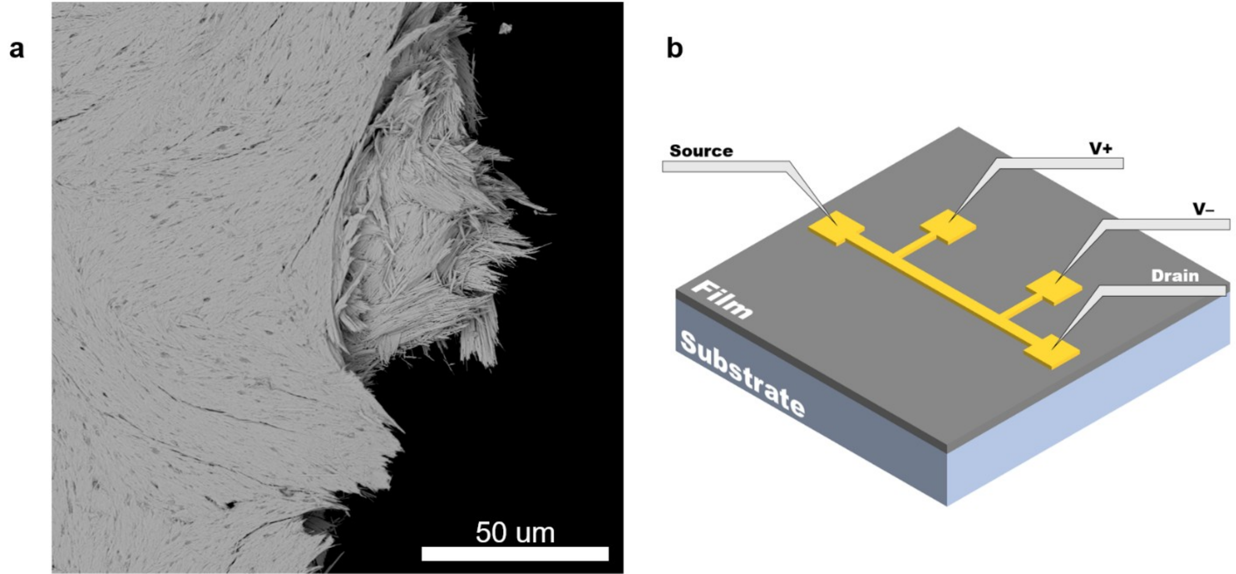

FIG 1. (a) SEM image of Te-PEDOT:PSS film (at a broken edge) showing its morphology. (b) Schematic of conventional 3-omega sample, used to measure the thermal properties of a film on a substrate. A heater line, acting as both a heater and sensor, is evaporated onto the measured film.

Volumetric heat capacity and cross-plane thermal conductivity measurement by model fit

To measure the volumetric heat capacity and cross-plane thermal conductivity of the film, we employ a common sample geometry used in 3ω (Fig 1b). That is, a film supported by the substrate (not suspended) with a heater evaporated onto it. Commonly, only in-phase temperature oscillations ($\Delta T_{in\text{-}phase}$) are analyzed and are measured at lower frequencies, so that the thermal wavelength in the film is larger than the film thickness. In this regime, relevant models of heat dissipation simplify, and the thermal conductivity can be calculated independently of the heat capacity. The thermal wavelength within a material defines the length scale upon which heat is dissipated in the system.

$$\lambda = \sqrt{k/2\omega C_v} \tag{0}$$

In this work, we measure ΔT over a much broader range of frequencies than commonly used and analyse both the in-phase and out-of-phase temperature oscillations. By extending our measured frequency range to include higher frequencies, where the thermal wavelength is commensurate with the film thickness, we gain sensitivity to the volumetric heat capacity of the film. However, we must fit our measured data to more complex models in order to calculate C_v and $k_{cross\text{-}plane}$. Here, we pair that measurement with a conventional 3ω analysis for comparison. We also compare our heat capacitance results to measurements obtained by MDSC[14].

Our sample film was produced by drop casting an aqueous solution of PEDOT:PSS-Te material onto a glass substrate. The resulting film has a thickness of 6.5 μm, measured by stylus profilometer. The heater was then thermally evaporated onto the film using a shadow mask, having nominal width 250 μm, and length 4 mm (Fig 1b). Due to the low electrical conductivity of our films (10 S/m), we do not need an

electrically insulating layer between the film and heater. The sheet resistance of the film is 15 kΩ/□, over 3 orders of magnitude higher than the heater resistance, such that any electrical transport through the film itself has a negligible effect on the measured voltage across the heater. Additionally, we fabricated a reference sample, which consists of an identical heater and substrate, but lacking a film between them. The reference sample allows us to isolate and measure the substrate properties, which are needed for modelling the behaviour of the film on substrate system. These samples are measured under high vacuum in a 4-probe configuration at room temperature. We measure our samples using a logarithmically spaced set of current frequencies from 0.1 Hz to 10 kHz.

The measured heater oscillation is fit to a 2-D conduction model of a multi-layer film supported by a substrate[7]. This model has generally been used to evaluate the errors associated with more conventional 3ω measurement approaches, as it is more accurate than commonly used models of heat conduction. More recently, it has been used to measure the thermal anisotropy of a film, $k_{in\text{-}plane}/ k_{cross\text{-}plane}$[22]. However in this work, we opt to measure $k_{in\text{-}plane}$ separately using a suspended sample, which is inherently more sensitive to in-plane conduction. In this work, we apply the 2-D model to measure the film's cross-plane thermal conductivity and volumetric heat capacity, but in principle it could be used to measure a variety of sample parameters, including film thicknesses and heater width as well.

In their publication, Borca-Tascuic et al. provide a general formula for the thermal impedance, Z, of a substrate with N films on it[7]:

$$\Delta T = ZP = \left(\frac{-1}{\pi l k_{y,N}} \int_0^\infty \frac{1}{A_N B_N} \frac{\sin^2(b\lambda)}{(b\lambda)^2} d\lambda \right) P \qquad (0)$$

$$A_i = \frac{A_{i-1}\frac{k_{y,i-1} B_{i-1}}{k_{y,i} B_i} - \tanh\left(B_i d_i\right)}{1 - A_{i-1}\frac{k_{y,i-1} B_{i-1}}{k_{y,i} B_i}\tanh\left(B_i d_i\right)},\ i \geq 1 \qquad (0)$$

$$A_0 = -1/\tanh\left(B_0 d_0\right) \qquad (0)$$

$$B_i = \left(k_{xy,i}\, \lambda^2 + \frac{i\, 2\omega}{\alpha_{y,i}} \right)^{1/2} \qquad (0)$$

$$\alpha_{y,i} = k_{y,i} / C_{v,i} \qquad (0)$$

The thermal impedance, Z, relates the amplitude of temperature oscillation of the wire, ΔT, to the amplitude of power oscillation, P, both at frequency 2ω. Z is complex, imparting both real and imaginary components to ΔT, which correspond to the in-phase and out-of-phase components of the oscillation,

respectively. The index, i, refers to the layer number counting upward from the substrate (i=0). k_{yi} refers to the cross-plane thermal conductivity of layer i ($\vec{y}$ is oriented perpendicular to the film, $\vec{x}$ is in-plane), $C_{v,I}$ is the layer volumetric heat capacity, $\alpha_{y,i}$ is the cross-plane diffusivity, and $k_{xy}= k_{in\text{-}plane}/ k_{cross\text{-}plane}$, the thermal conductance anisotropy. d_i is the layer thickness, b is the heater half-width, and l the heater length. A_i and B_i are place holder variables to aid readability, with each A_i defined by A_{i-1}, except for that pertaining to the bottom layer (substrate) A_0. Here, we define A_0 for the isothermal condition on the substrate bottom, which means that thermal excitations are completely attenuated at the bottom edge of the substrate. In their publication, Borca-Tascuic et al. provide alternate definitions of A_0 for insulated and infinite bottom edges as well, which we are in the SI along with a diagram of this 2D conduction model. The model most closely matches our data for the isothermal condition, likely because the substrate is adhered to a copper block with high thermal conductivity. None of these conditions perfectly match experimentally realizable behaviour, which causes the model to diverge from experiment at too low a frequency (Fig. 2a-c).

Another limitation of this model is that it disregards the thermal mass of the heater itself, which causes error at high heating frequencies. Higher frequencies are important for our purposes, as the thermal response of the heater is more sensitive to the film's heat capacity for shorter thermal wavelengths. Therefore, we use a modified thermal impedance, Z', for the system, which includes, G, the thermal impedance of the heater[7].

$$Z' = \left(Z^{-1} + G^{-1}\right)^{-1} \tag{0}$$

$$G^{-1} = i4\omega bl\, d_h C_{v,h} \tag{0}$$

G primarily includes the heater's volume, $V_h=2bld_h$, and its volumetric heat capacity, $C_{v,h}$. This formula assumes that the heater temperature remains uniform throughout its volume.

In order to fit our measured temperature data to this model, we use the non-linear least squares Gauss-Newton algorithm. This method makes iterative adjustments to the fitted parameters with the aim of minimizing the difference between the measured and modelled ΔT throughout a frequency range. This relies on the partial derivative of ΔT with respect to these parameters, but importantly, does not require an analytic solution for the intractable integral within the model; derivatives can be calculated analytically, and integrals computed numerically over large limits such that they converge. Our model for ΔT has 2 outputs at each frequency, the in-phase component and out-of-phase component ($Re(\Delta T)$ and $Im(\Delta T)$ respectively). So if we are fitting data from M discrete frequencies, that becomes 2M real-valued functions of the model. Using this method, we measure the thermal conductivity and heat capacity of the film and substrate by fitting those parameters to measured data.

Our initial analysis is of the reference sample, the bare glass substrate. As with more conventional 3-omega approaches, we must carefully consider the applicable frequency domain of our model. We pick a lower frequency limit, f>0.57 Hz, to maintain a thermal wavelength within the glass substrate to be less than half the substrate thickness ($\lambda<d_{sub}/2$), which minimizes influence from the substrate bottom which the model does not perfectly account for[8,23]. Our upper frequency limit is f<3 kHz, chosen to avoid data affected by an electrical resonance in our measurement system at higher frequencies.

Fitting measured data to our model within these frequency bounds, we measure the thermal conductivity of the glass substrate to be 1.05 W/mK, and its volumetric heat capacity to be 1.96 x 10^6 J/m^{3}K (Fig. 2a). We use N=0 in the model, as there are no films present. Other model parameters, such as the exact heater width and substrate thickness, are measured independently.

The conventional method for measuring isotropic bulk materials, is to fit their in-phase temperature oscillations to a line in order to extract the slope $dT_{in\text{-}phase}/d(\ln \omega)$[5,8]. Over a specific frequency range, this slope is inversely proportional to the thermal conductivity of the material. Using this line fitting analysis, we measure a thermal conductivity of 1.06 W/mK. For this measurement, we use a thinner heater, with width 46 µm, to better accommodate the simplified model this method relies on. Using MDSC, we measure the volumetric heat capacity of the substrate to be 1.91 x 10^6 J/m^{3}K. Clearly, both the thermal conductance and volumetric heat capacity of the glass substrate, measured through curve fitting, match these conventional measurements. They also match values provided by the substrate manufacturer, k=1.09W/mK and C_v=1.81 x 10^6 J/m^{3}K, for alkaline earth boro-aluminosilicate glass (EAGLE XG, Corning) at room temperature[24].

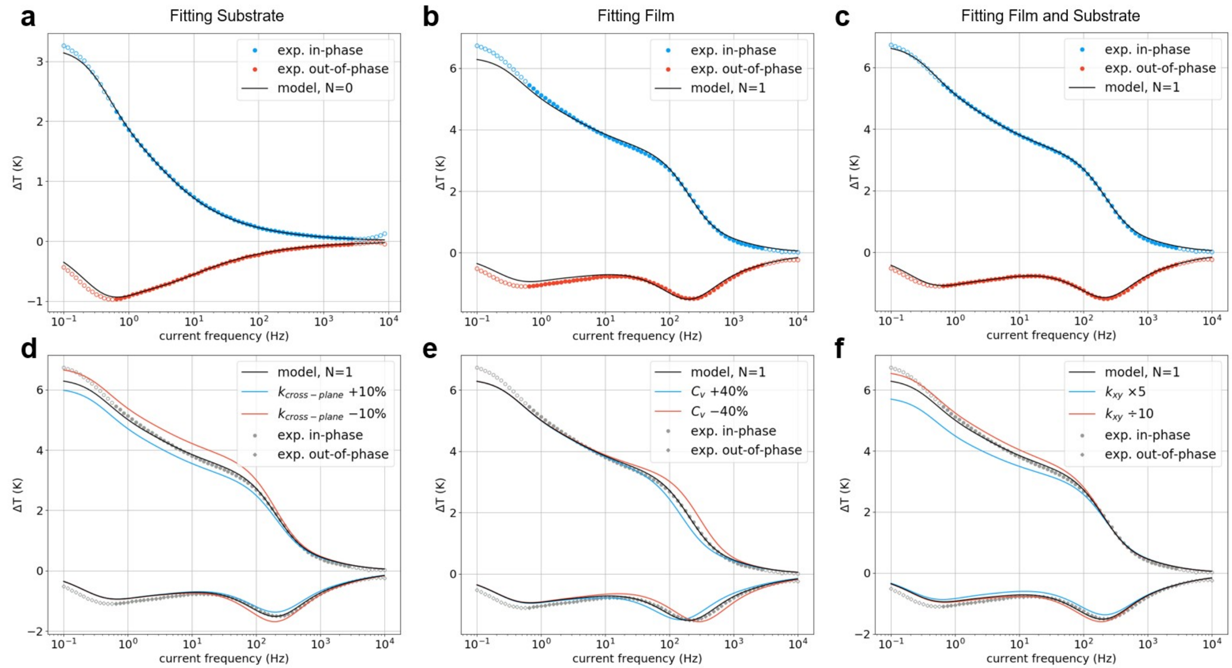

FIG. 2. Fitting film on substrate data to model (a) Measurement of reference device to determine substrate properties, k_{sub}, and $C_{v,\,sub}$, by fitting measured 3ω temperature oscillation, ΔT, to our model. Only the filled data points are used in the fit. (b) Measurement of film properties, $k_{cross\text{-}plane}$ and $C_{v,\,film}$, by model fit. The substrate values determined in (a) are used as parameters for the fit. (c) Measurement of both substrate and film properties simultaneously by allowing all 4 parameters to change. (d,e,f) effect of varying model parameters, $k_{cross\text{-}plane}$, $C_{v,\,film}$, and $k_{xy,\,film}$ starting from the best fit determined in (b).

We use a similar model fitting technique for our measurement of the Te-PEDOT:PSS film's thermal properties using the film-on-substrate sample. We use the single-film variation of our model

(N=1), and utilize the measured substrate thermal properties ($k_{substrate}$ and $C_{v,\ substrate}$) as model inputs. By model fitting, we measure the film's cross-plane thermal conductivity as 3.0 x 10^{-2} W/mK and volumetric heat capacity as 5.1 x 10^5 J/m^{3}K (Fig. 2b).

The conventional 3ω approach to measuring the film's cross plane thermal conductivity, is the differential method[8,25]. The in-phase temperature oscillation of the film-on-substrate is measured and compared against that of the reference sample. Their difference is used to calculate the cross-plane thermal conductivity of the film. Using this standard differential method, we measure $k_{cross\text{-}plane}$=3.3 x 10^{-2} W/mK, which agrees with our curve fitting analysis within 10%. By MDSC, we measure the volumetric heat capacity of PEDOT:PSS-Te films as 6.6 x 10^5 J/m^{3}K, which differs from our curve fitting analysis by 30%. However, MDSC only provides the specific heat capacity; the determination of the film's volumetric heat capacity requires a separate measurement of the density, which is itself difficult and prone to error for light, thin films. By contrast, this 3ω model fitting approach directly measures the film's volumetric heat capacity.

An alternative model fitting analysis is to measure multiple layers simultaneously. If $k_{cross\text{-}plane}$ and C_v of both the film and substrate are measured, there are 4 total fitting parameters (Fig. 2c, Table 1). This analysis eliminates the need for a bare substrate reference and results in modeled data which very closely matches the measured data. However, as more parameters are allowed to fit the model, the resulting accuracy, especially for properties of buried layers, becomes suspect. For example, this method results in substrate conductivity of $k_{substrate}$=0.91 W/mK, which differs considerably from our other measurements. While less accurate, this method of fitting multiple film properties simultaneously may still prove valuable where otherwise separating layers is impossible. Another potential variation of this technique, is using the N=2 variant of the model in cases where an electrically insulating layer resides between the heater and measured film. In this scenario, properties of the insulation layer can be measured as fitting parameters, or supplied to the model for more accurate results.

Sample	**Method**	**k_{sub} (W/mK)**	**$C_{v,\ sub}$ (J/m^{3}K)**	**$K_{cross\text{-}plane,\ film}$ (W/mK)**	**$C_{v,\ film}$ (J/m^{3}K)**
bare substrate	model fitting (sub. only, Fig 2a)	1.05	1.96 x 10^6		
film on substrate	model fitting (film only, Fig 2b)			3.0 x 10^{-2}	5.1 x 10^5
film on substrate	model fitting (film and substrate, Fig 2c)	0.91	1.75 x 10^6	3.1 x 10^{-2}	4.8 x 10^5
bare substrate	slope of $T_{in\text{-}phases}$	1.06			
film on sub. and bare	differential			3.3 x 10^{-2}	
testing pan	MDSC		1.91 x 10^6		6.6 x 10^5

Table 1. The thermal conductivities and heat capacities measured by alternate means for comparison.

A limitation of this model is that it does not directly account for interfacial thermal resistances between layers. While it can be altered to include a boundary resistance between the heater and top layer[7], there is no straightforward correction for resistances between layers, i.e. the film and glass substrate. By measuring an alternative device of lesser thickness (5.2 um), we can obtain a rough estimate of unaccounted thermal resistances in the system using a differential technique with a linear regression[6,8]. We estimate boundary resistances Rc 8 x 10^{-6} m^2K/W in the system, which contributes a 4% error in the determination of $k_{cross\text{-}plane}$. This model fitting method is more reliable in systems like ours where the thermal resistance of the film itself is much larger than these unaccounted for boundary resistances ($d_{film}/k_{cross-plane} \gg R_c$).

As we can see from Fig 2d-f, different frequency regions of the temperature oscillation are sensitive to different film parameters. The in-phase temperature oscillation is more sensitive to $k_{cross\text{-}plane}$ of the film at lower frequencies. Conversely, C_v primarily affects higher frequency temperature excitations, both in-phase and out-of-phase, in a region centered around $d_{film} \approx \lambda_{cross-plane}$, where the cross-plane thermal wavelength within the film matches the film thickness. At these high frequencies, the induced temperature wave resides primarily in the film, not the substrate, so that the wave dynamics are strongly affected by the thermal mass of the film[26,27]. Therefore, a measurement of heat capacity must include this section of the frequency domain. Moreover, in instances where thicker films may disqualify the differential 3ω method, due to strict frequency requirements[8,25], this model fitting approach is still valid.

Since we use a wide heater, our measurements are insensitive to the anisotropy of the sample, $k_{xy}= k_{in\text{-}plane}/ k_{cross\text{-}plane}$ (Fig. 2f). Specifically, our heaters are much wider than the film thickness, $2b/d_{film}=40$. While there is some in-plane conduction at the heater edge, the wide heater ensures that most conduction will happen in the cross-plane direction directly under the heater[8]. For our purposes, this is ideal, since it makes our measurements insensitive to the in-plane thermal conductivity, expressed in the model as an anisotropy factor, k_{xy}. We use an estimated anisotropy of $k_{xy}=20$ as a fitting parameter, which looking forward at our $k_{in\text{-}plane}$ results, has a 5% error. This error in anisotropy only affects our measured values of $k_{cross\text{-}plane}$ and C_v by 0.2% and 0.1% respectively, due to this insensitivity. Using a wide heater, one can accurately measure the film's cross-plane conductivity and heat capacity using this model fitting method with only a reasonable estimate of the film anisotropy. If one wishes to apply this method to measure the anisotropy, then much thinner heater lines are required to achieve greater sensitivity to k_{xy}, likely requiring more advanced microfabrication than shadow masking[22]. For our measurement of the film's in-plane thermal conductivity, we opt for the suspended film technique, as it is inherently more sensitive to in-plane thermal conduction than using a supported film geometry.

Suspended in-plane thermal conductivity measurement via embedded micro-wire

To measure the in-plane thermal conductivity of the film, we use a suspended sample geometry, which requires a different model of conduction. In this geometry, we can approximate heat conduction using a 1-D model, wherein heat travels purely in-plane with the film, perpendicularly outward from the heater[11]. The measurement is very sensitive to in-plane thermal conduction, while only requiring a single sensor, the heater. This requires a relatively thin heater, thinner than the in-plane thermal wavelength of the film for accurate results. Fabricating a thin heater by thermal evaporation can be overly challenging on a suspended film, especially one such as Te-PEDOT:PSS which is rough and water-soluble. Instead of an evaporated heater, we have developed the use of a thin Pt micro-wire heater, embedded into a drop cast film (Fig. 3). This Pt wire has 12 μm diameter, but is highly conductive and has a high thermal coefficient

of resistance[28], which is necessary for its temperature sensing capability. The Pt wire was purchased by California Fine Wire Co.

We fabricate our films by drop casting aqueous Te-PEDOT:PSS onto a PTFE substrate, which enables delamination after drying. Prior to drop casting, we secure the heater wire onto the PTFE substrate in a 4-probe configuration so that the film encases it (Fig. 3c). Optical images show that the drop cast material completely envelopes the Pt heater line (Fig. 3b) ensuring an intimate thermal connection. Though the voltage probe wires merely cross the heater wire, making surface contact, they exhibit contact resistances less than 10 ohms after drying. After preparation, the films are supported at the edges by sapphire substrates, keeping the measured region suspended (Fig. 3a). Samples are measured at high vacuum in a 4 probe configuration at room temperature.

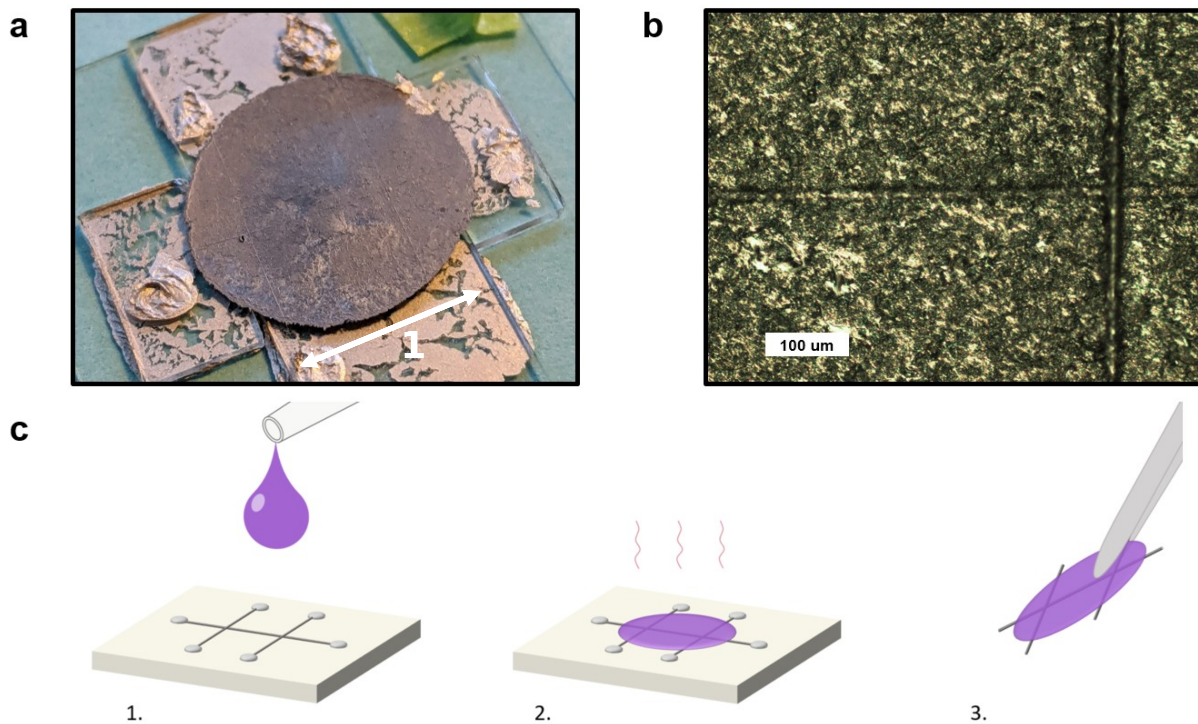

FIG. 3. Sample preparation (a) Image of a suspended film used for in-plane measurement. A faintly visible Pt micro-wires run through the film in a 4-probe configuration. (b) Image of two embedded wires crossing within the film, both completely encased in material. (c) Construction of suspended film sample 1. Pt micro-wire is affixed to a PTFE substrate using silver paste at it ends. 2. The material is drop cast onto the substrate and baked. 3. The film and embedded wire are carefully peeled from the substrate.

Since our heater is now embedded into the film, rather than resting atop it, the 2-D model of heat conduction used in the previous section is not valid. Fortunately, heat conduction in a thin suspended film is relatively simple, as heat is forced to travel almost entirely in-plane within our measured frequency range. Therefore, we analyze the measured temperature oscillations through a simple 1-D model of thermal conduction[11].

$$\Delta T_{1D} = \frac{P}{2\,dl\sqrt{2\,\omega\,C_v\,k_{¿-plane}}}\,e^{\frac{-i\pi}{4}}$$

(0)

As in the previous 2-D model, ΔT is the amplitude of temperature oscillation in the wire, and is proportional to P, the AC power induced by the heater. d is the film thickness and C_v is the film's volumetric heat capacity. We can therefore calculate the in-plane thermal conductivity as:

$$k_{¿-plane} = \frac{P^2}{8\,C_v\,l^2\,d^2}\left(\frac{d\left|\Delta T\right|}{d\left(\omega^{-1/2}\right)}\right)^{-2}$$

(0)

In the valid region of our model, we can simply fit ΔT to a line and use the slope to calculate $k_{in\text{-}plane}$ (Fig. 4b). However, unlike other of 3ω methods, we need a separate measure of the films volumetric heat capacity, which in this case is supplied by the previously discussed model fitting method on a supported film.

This simple 1-D model assumes that the film has a negligible thickness, that no heat is lost through the film surfaces, and that the film and heater extend infinitely far. To minimize error arising from the film thickness, we impose a condition between the film thickness and thermal wavelength, $d/\lambda_{cross\text{-}plane}<0.4$[11], which limits our frequency space to f < 3.3 Hz. In principle, we must also ensure that the heater width is negligible as well, but fortunately the micro-wire heater is much thinner than relevant length scales.

The lower frequency limit of the measurement can arise from different constraints depending on the sample, but in this case, we found that the onset of heat loss at the film surfaces by thermal radiation was the primary limiter. In conventional 3ω measurements, where the heater is supported by a bulk material, thermal radiation can generally be ignored, as the heat radiated by the top surface is insignificant compared to the heat dissipating down into the thick substrate. On a thin suspended film, however, heat can only dissipate outward, traveling along the film's surface. This leads to higher surface temperatures over a wider area around the heater, drastically increasing radiative losses at the film's two surfaces, especially at lower frequencies. In order to estimate the error induced by thermal radiation, we apply the Stefan-Boltzmann law to the film surfaces to calculate the effective heat loss density, q_{rad}, within the film.

$$q_{rad} = \frac{-8\,\epsilon\sigma T_{mean}^3}{d}\,T_{AC} = -v\,T_{AC}$$

(0)

Here q_{rad} specifically pertains to the AC component of radiative heat loss and is a first order approximation in T_{AC}, the temperature fluctuation of the film. This heat loss leads to an altered equation for the wire temperature (see SI):

$$\Delta T_{1D+rad} = \frac{P}{2\,dl\sqrt{k_{¿-plane}}\sqrt{i\,2\,\omega\,C_v + v}}$$

(0)

As ω is reduced, the role of thermal radiation, as expressed by ν, has a larger effect on the wire temperature. Physically, as the frequency lowers, temperature oscillations within the film grow, increasing the heat lost to surface radiation. The thermal wavelength also lengthens at lower frequencies, widening the radiative surface area of the film. Our measured wire temperature closely matches this radiative model if we use an emissivity, $\epsilon = 0.44$, for the film surface (Fig 4a).

For the purposes of measuring $k_{in\text{-}plane}$, we wish to find a frequency range in which heat loss has a minor effect. We calculate the relative error the $k_{in\text{-}plane}$ measurement, due to radiation:

$$\Re\left(k_{¿-plane}\right)=\frac{5}{8}\left(\frac{\nu}{\omega C_v}\right)^2=40\left(\frac{\epsilon\sigma T_{mean}^3}{d\omega C_v}\right)^2 \qquad (0)$$

By targeting an error of 5%, we obtain the condition f > 0.93 Hz. For this calculation we use a maximal surface emissivity, $\epsilon = 1$, so that we do not underestimate the error. Depending on the parameters of the sample, the minimum frequency may also be defined by the heater length, and the lateral dimensions of the sample. Here, the in-plane thermal wavelength, $\lambda_{in\text{-}plane}$=309 μm at 0.93 Hz, which is an order of magnitude less than both the sample length (l=5.44 mm) and the distance from the heater to the sample edge (about 3.9mm), ensuring that the induced thermal excitation is unaffected by these dimensions. Indeed, the onset of radiative losses at low frequencies is the chief limiter of the frequency range for the measurement of our suspended films.

Through the line fit, we calculate the film's thermal conductivity as $k_{in\text{-}plane}$=0.57 W/mK (Fig 4b). We therefore measure an anisotropy of $k_{in\text{-}plane}/ k_{cross\text{-}plane}$=19. For this measurement, we rely on our model fitting results for the volumetric heat capacity. The thickness of the suspended film is measured after the 3ω measurement. We re-wet and dry the film onto a substrate so that we can get an accurate measure of its thickness by stylus profilometer (d=15.0 μm).

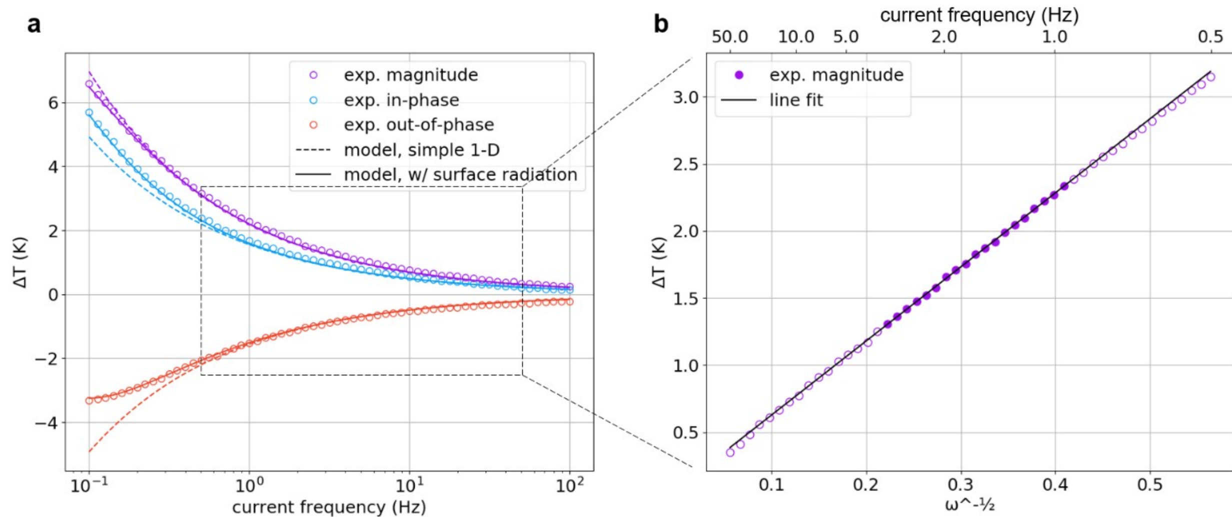

FIG. 4. In-plane thermal conductivity measurement. (a) The measured temperature excitation in the suspended sample, compared against the simple 1-D conduction model and our model with radiative

cooling. We choose the model emissivity, $\epsilon = 0.44$, to better match our data. (b) $|\Delta T|$ measured against $\omega^{-1/2}$. The slope is taken in the most valid region (filled markers) to measure $k_{in\text{-}plane}$.

Conclusions

As expected, we measure a large anisotropy in our Te-PEDOT:PSS films, of $k_{in\text{-}plane}/k_{cross\text{-}plane}=19$. We also measure a very low volumetric heat capacity of 5.1 x 10^5 J/m^{3}K, which is lower than both constituent materials, bulk Tellurium (1.3 x 10^6 J/m^{3}K)[15] and PEDOT:PSS (~2 x 10^6 J/m^{3}K)[16]. This indicates that the nanowire mesh forming our films contains many voids. This void space likely lowers the thermal conductance in all directions, especially for these measurements under vacuum. However, the nanoscale morphology of these films results in an especially low cross-plane conductivity. The thermal properties of composite nanostructured materials such as Te-PEDOT:PSS are non-trivial and require new measurement techniques to be measured more easily.

Here we have demonstrated two measurement techniques which together, can provide a comprehensive measurement of a films thermal properties. The use of model fitting for the extraction of volumetric heat capacity of a supported film is itself a powerful technique and could be applied to other films which are difficult to measure separately, such as epitaxially grown materials or multilayer stacks. More generally, the development of 3ω techniques which do not rely on advanced lithography and can be applied to a broader array of materials will ease the material discovery process.

Supplementary Material

See supplementary material for more complete description of the 2-D thermal conduction model and derivation of the 1-D model with thermal radiation.

Acknowledgements

We thank Professor Chris Dames and his research group for their advice and support. This work was performed at the Molecular Foundry, Lawrence Berkeley National Laboratory, and was supported by the Department of Energy, Office of Science, Office of Basic Energy Sciences, Scientific User Facilities Division of the U.S. Department of Energy under contract no. DE-AC02-05CH11231. M.P.G. acknowledges the NSF for fellowship support under the NSF Graduate Research Fellowship Program.

Competing Interests

The authors have no conflicts to disclose.

[1] H. Wang, W. Chu, and G. Chen, Adv. Electron. Mater. **5**, 1900167 (2019).

[2] D.G. Cahill, P. V. Braun, G. Chen, D.R. Clarke, S. Fan, K.E. Goodson, P. Keblinski, W.P. King, G.D. Mahan, A. Majumdar, H.J. Maris, S.R. Phillpot, E. Pop, and L. Shi, Appl. Phys. Rev. **1**, 011305 (2014).

[3] P. Jiang, X. Qian, and R. Yang, J. Appl. Phys **124**, 161103 (2018).

[4] X. Xu, J. Chen, J. Zhou, and B. Li, Adv. Mater. **30**, 1705544 (2018).

[5] D.G. Cahill, Rev. Sci. Instrum. **61**, 802 (1990).

[6] J.H. Kim, A. Feldman, and D. Novotny, J. Appl. Phys. **86**, 3959 (1999).

[7] T. Borca-Tasciuc, A.R. Kumar, and G. Chen, Rev. Sci. Instrum. **72**, 2139 (2001).

[8] C. Dames, Annu. Rev. Heat Transf. **16**, 7 (2013).

[9] A. Jain and K.E. Goodson, J. Heat Transfer **130**, 102402 (2008).

[10] N. Bodenschatz, A. Liemert, S. Schnurr, U. Wiedwald, and P. Ziemann, Rev. Sci. Instrum. **84**, 084904 (2013).

[11] S. Kommandur and S. Yee, Rev. Sci. Instrum. **89**, 114905 (2018).

[12] X. Zhang and C.P. Grigoropoulos, Rev. Sci. Instrum. **66**, 1115 (1995).

[13] V. Mishra, C.L. Hardin, J.E. Garay, and C. Dames, Rev. Sci. Instrum. **86**, 054902 (2015).

[14] E. Verdonck, K. Schaap, and L.C. Thomas, Int. J. Pharm. **192**, 3 (1999).

[15] D. Medina-Cruz, W. Tien-Street, A. Vernet-Crua, B. Zhang, X. Huang, A. Murali, J. Chen, Y. Liu, J. Miguel Garcia-Martin, J.L. Cholula-Díaz, and T. Webster, in *Racing Surf. Antimicrob. Interface Tissue Eng.* (Springer, Cham, 2020), pp. 723–783.

[16] J. Liu, X. Wang, D. Li, N.E. Coates, R.A. Segalman, and D.G. Cahill, Macromolecules **48**, 585 (2015).

[17] A.K.K. Kyaw, T.A. Yemata, X. Wang, S.L. Lim, W.S. Chin, K. Hippalgaonkar, and J. Xu, Macromol. Mater. Eng. **303**, 1700429 (2018).

[18] M.P. Gordon, K. Haas, E. Zaia, A.K. Menon, L. Yang, A. Bruefach, M.D. Galluzzo, M.C. Scott, R.S. Prasher, A. Sahu, and J.J. Urban, Adv. Electron. Mater. **7**, 2000904 (2021).

[19] L. Yang, M.P. Gordon, A.K. Menon, A. Bruefach, K. Haas, M.C. Scott, R.S. Prasher, and J.J. Urban, Sci. Adv. **7**, (2021).

[20] N. Mehra, L. Mu, T. Ji, X. Yang, J. Kong, J. Gu, and J. Zhu, Appl. Mater. Today **12**, 92 (2018).

[21] K. Ruan, X. Shi, Y. Guo, and J. Gu, Compos. Commun. **22**, 100518 (2020).

[22] D. Singhal, J. Paterson, D. Tainoff, J. Richard, M. Ben-Khedim, P. Gentile, L. Cagnon, D. Bourgault, D. Buttard, and O. Bourgeois, Rev. Sci. Instrum. **89**, 084902 (2018).

[23] A. Jacquot, B. Lenoir, A. Dauscher, M. Stölzer, and J. Meusel, J. Appl. Phys. **91**, 4733 (2002).

[24] Corning Incorporated, *Eagle XG Product Information* (2021).

[25] D.G. Cahill, M. Katiyar, and J.R. Abelson, Phys. Rev. B **50**, 6077 (1994).

[26] Y.S. Ju, K. Kurabayashi, and K.E. Goodson, Microscale Thermophys. Eng. **2**, 101 (1998).

[27] Y.S. Ju and K.E. Goodson, J. Appl. Phys. **85**, 7130 (1999).

[28] R. Karthik, N. Harish Nagarajan, B. Raja, and P. Damodharan, J. Eng. Thermophys. **21**, 60 (2012).